

Standard Grids for High-Precision Integration of Modern Density Functionals: SG-2 and SG-3

Saswata Dasgupta and John M. Herbert *

Density-functional approximations developed in the past decade necessitate the use of quadrature grids that are far more dense than those required to integrate older generations of functionals. This category of difficult-to-integrate functionals includes meta-generalized gradient approximations, which depend on orbital gradients and/or the Laplacian of the density, as well as functionals based on B97 and the popular “Minnesota” class of functionals, each of which contain complicated and/or oscillatory expressions for the exchange inhomogeneity factor. Following a strategy introduced previously by Gill and co-workers to develop the relatively sparse “SG-0” and

“SG-1” standard quadrature grids, we introduce two higher-quality grids that we designate SG-2 and SG-3, obtained by systematically “pruning” medium- and high-quality atom-centered grids. The pruning procedure affords computational speedups approaching a factor of two for hybrid functionals applied to systems of ~ 100 atoms, without significant loss of accuracy. The grid dependence of several popular density functionals is characterized for various properties. © 2017 Wiley Periodicals, Inc.

DOI: 10.1002/jcc.24761

Introduction

Density functional theory (DFT), the most widely-used electronic structure method due to its relatively low cost and often predictive accuracy, continues to evolve. New and better exchange-correlation functionals are introduced every year, and these functionals can generically be written as

$$E_{xc}[\rho_\alpha, \rho_\beta] = \int d\mathbf{r} F(\rho_\alpha, \rho_\beta, \hat{\nabla} \rho_\alpha, \hat{\nabla} \rho_\beta, \dots). \quad (1)$$

This integral must be evaluated by numerical quadrature. For this purpose, concentric atom-centered Lebedev^[1,2] integration grids are the standard approach.^[3] These may be specified using a notation (N_r, N_Ω) that indicates the number of radial shells for each atom, N_r , and the number of angular (Lebedev) points for each shell, N_Ω . The original “standard grid” (SG-1) introduced by Gill et al.^[4] in 1993 is based on a (50,194) quadrature that was then further “pruned” by removing some angular points near the nuclei, where the density is locally spherically-symmetric, and also far from the nuclei, where the density varies slowly. The SG-1 grid is accurate and efficient for what was state-of-the-art DFT in the late 1990s, for example, application of B3LYP/6-31G* to bonded systems.

It is increasingly clear, however, that the SG-1 grid is *not* adequate for many of the new density-functional approximations developed in the past decade.^[5–12] In particular, meta-generalized gradient approximations (meta-GGAs), in which the functional F in eq. (1) depends on the kinetic energy density

$$\tau_\sigma(\mathbf{r}) = \sum_i |\hat{\nabla} \psi_{i,\sigma}(\mathbf{r})|^2 \quad (2)$$

and/or the Laplacian of the density ($\hat{\nabla}^2 \rho_\sigma$), tend to be more sensitive to the quality of the integration grid. Many newer

functionals, including the popular “Minnesota” suite of functionals, developed by Truhlar and coworkers since 2005,^[13,14] also contain relatively complicated expressions for the exchange and correlation inhomogeneity factors, rendering them more demanding to integrate.^[15] As non-local density functionals that can properly describe non-covalent interactions have begun to appear,^[10,11,16–19] it has also been discovered that these interactions converge very slowly with respect to the integration grid,^[7,8,10,11,15] because non-covalent interactions are characterized by large density gradients in regions where the density itself is small.^[20] Spurious oscillations in potential surfaces can arise when the grid is too sparse,^[7,8] as shown for argon dimer in Figure 1, using four density functionals developed since 2006.

Although references to pruned versions of grids denser than SG-1 can be found in the literature,^[21] and in the online documentation for the GAMESS^[22] and GAUSSIAN^[23] programs, the grid points themselves have not been published. As such, these cannot constitute *standard* integration grids that can be used to make comparisons and validations between electronic structure codes, at the level of machine precision. Quantitative tests of the impact of the pruning procedure on molecular properties are also lacking, such that there is no single source in the literature to understand the impact of grid pruning on a large swath of molecular properties.

S. Dasgupta, J. M. Herbert

Department of Chemistry & Biochemistry, The Ohio State University, Columbus, Ohio 43210 E-mail: herbert@chemistry.ohio-state.edu

Contract grant sponsor: U.S. Department of Energy, Office of Basic Energy Sciences, Division of Chemical Sciences, Geosciences, and Biosciences; Contract grant number: DE-SC0008550; Contract grant sponsor: National Science Foundation; Contract grant number: CHE-1300603; Contract grant sponsor: Alexander von Humboldt Foundation (to J.M.H.)

© 2017 Wiley Periodicals, Inc.

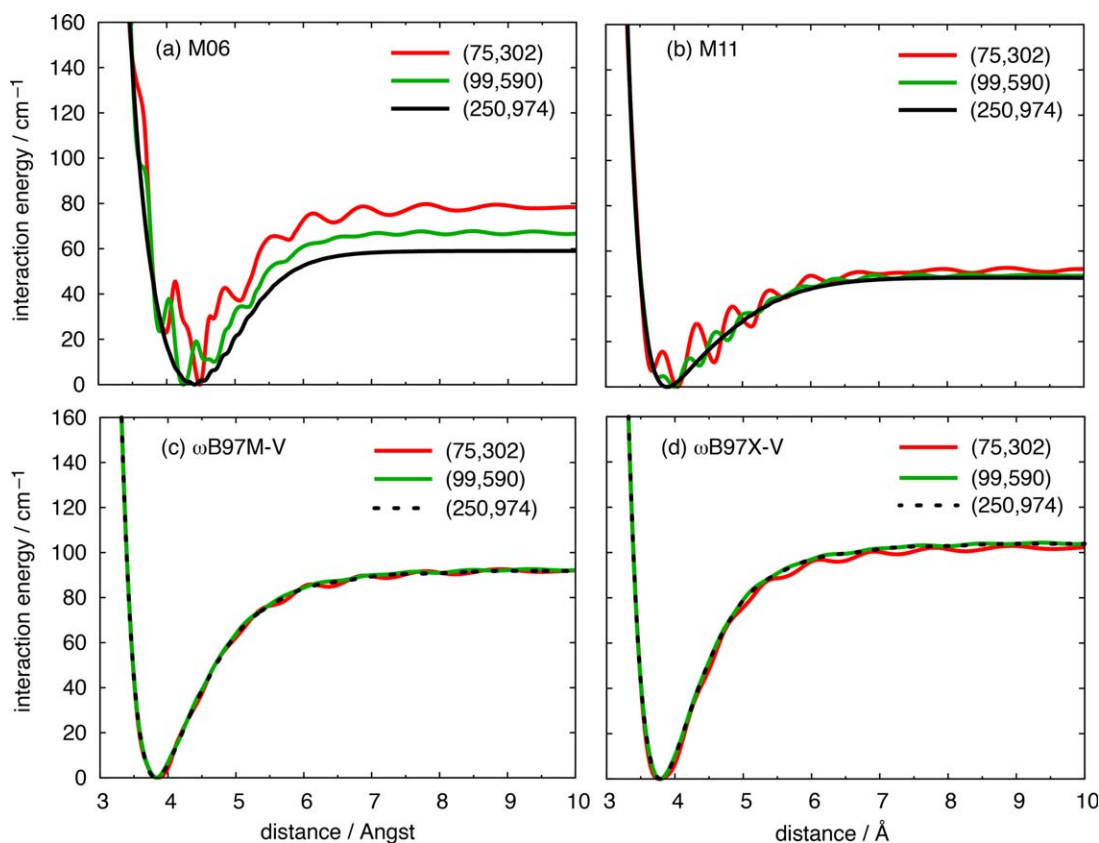


Figure 1. Potential energy curves for Ar_2 using various integration grids for the density functionals (a) M06, (b) M11, (c) $\omega\text{B97M-V}$, and (d) $\omega\text{B97X-V}$, using the aug-cc-pVTZ basis set in each case. For M06, not even the extremely dense (250,974) grid is free of spurious oscillations. Results for the two B97-based functionals with the (99,590) grid exhibit very small oscillations that are barely visible on the scale of the figure, as compared to the (75,302) grid where small undulations are apparent, but the (250,974) potential energy curves are free of any oscillations whatsoever. [Color figure can be viewed at wileyonlinelibrary.com]

In view of this situation, we decided to develop and test the next generation of pruned integration grids: SG-2 and SG-3. These are pruned versions of a (75,302) and a (99,590) quadrature grid, respectively, as these two choices of (N_r, N_Ω) have been shown to constitute grids of medium and high quality, respectively, even for modern functionals.^[10,11] Note that $75 \times 302 = 22,650$ grid points per atom is a *significant* increase relative to the SG-1 grid, which consists of 3816 points for each carbon nucleus, for example. To reduce the cost, we follow the pruning procedure of Gill and co-workers,^[4,24] removing some of the angular points in each radial shell, in a systematic way, stopping before the quality of the integration becomes unacceptable.

The SG-2 grid introduced here contains just 31–39% of the 75×302 grid points that one would anticipate, depending on the particular nucleus in question, and SG-3 contains just 25–33% of 99×590 grid points, yet the pruned grids are accurate to within a few $\mu\text{Hartree}$ of the original, unpruned grids, and errors in energy differences and molecular properties are quite small on chemically-relevant scales, as documented herein. Reduction in the number of grid points translates immediately into a reduction in cost, as each of the quantities on which the function F depends must be evaluated at each grid point and at each self-consistent field (SCF) iteration.

Theory

Due to the electron density cusp at each nucleus, Cartesian grids are not ideal for molecular integrals. Instead, the standard approach is Becke's partitioning scheme,^[25] in which the molecular integral is approximated as a sum of atomic sub-integrals, each of which is then evaluated by quadrature in spherical polar coordinates. The quadrature amounts to

$$\int_0^\infty r^2 dr \int_0^\pi \sin \theta d\theta \int_0^{2\pi} d\phi F(r, \theta, \phi) \approx \sum_{i=1}^{N_r} w_i^r \sum_{j=1}^{N_\Omega} w_j^\Omega F[\rho(r_i, \theta_j, \phi_j)], \quad (3)$$

with radial weights w_i^r and angular weights w_j^Ω . The angular part of the sum represents integration over the surface of a sphere, which can be performed efficiently via the Lebedev scheme.^[1,2] The latter is an exact quadrature for functions

$$f(\theta, \phi) = \sum_{\ell=0}^{\ell_{\max}} \sum_{m=-\ell}^{\ell} c_{\ell m} Y_{\ell m}(\theta, \phi) \quad (4)$$

that can be expressed as linear combinations of a finite number of spherical harmonics. For example, the 302-point Lebedev grid

that we use for SG-2 will integrate f exactly if $\ell_{\max} \leq 29$, and for the 590-point SG-3 grid it is $\ell_{\max} \leq 41$.

This leaves open the question of the radial quadrature, for which various schemes have been used.^[24,26–31] The SG-1 grid uses the Euler–Maclaurin scheme,^[4,26] but for the subsequent SG-0 grid, a “MultiExp” quadrature was developed that is more efficient for integrating linear combinations of Gaussian functions.^[24] Unlike some other quadrature schemes in which there are analytic expressions for the locations of the quadrature points, however, in the MultiExp approach these nodes must be obtained by solving a set of linear equations that becomes increasingly ill-conditioned as the number of grid points increases. Due to numerical problems associated with this ill-conditioning, we were unable to extend the MultiExp approach to the desired high-quality value, $N_r = 99$. In the interest of consistency between SG-2 and SG-3 (and possible extension to even denser grids at some later time), we therefore choose the “double exponential” scheme for the radial quadrature, also known as the “tanh-sinc” quadrature.^[30–33] For N grid points, this promising approach exhibits an error of $\mathcal{O}[\exp(-N/\log N)]$, and it has been proven that the error estimation of the trapezoidal integration formula with equal mesh size is optimal for numerical integration of an analytic function over the interval $(-\infty, +\infty)$.^[32] This is a faster decay rate in the error, with respect to N , as compared to other known quadratures.^[30]

To use the double exponential quadrature over a finite interval $[a, b]$, this interval must be mapped onto $(-\infty, +\infty)$ by means of a transformation $y = t(x)$ ^[30]:

$$\int_a^b f(y) dy = \int_{-\infty}^{\infty} f(t(x)) \frac{dt(x)}{dx} dx \approx h \sum_i t'(x_i) f(t(x_i)). \quad (5)$$

Here, h is a uniform grid spacing on the interval $[a, b]$, with $a = t(-\infty)$ and $b = t(+\infty)$, and $x_i = ih$.^[30] Three different versions of the double exponential quadrature have been proposed,^[30,31] corresponding to different mapping functions $t(x)$. The one that we will use in SG-2 and SG-3 is called the “DE2” quadrature in Refs. 30 and 31, and uses the mapping

$$t(x) = \exp(\alpha x - e^{\alpha x}). \quad (6)$$

Inserting eq. (6) into eq. (5) affords the double-exponential quadrature formula

$$\int_0^{\infty} F(r) r^2 dr \approx h \sum_i \exp(3\alpha x_i - 3e^{-x_i})(\alpha + e^{-x_i}) f(r_i) \quad (7)$$

where the radial quadrature points are

$$r_i = \exp(\alpha x_i - e^{-x_i}) \quad (8)$$

with weights

$$w_i = \exp(3\alpha x_i - 3e^{-x_i})(\alpha + e^{-x_i}) h. \quad (9)$$

In the context of DFT, it has been observed that this particular quadrature requires fewer points to converge, as compared to

the other two double-exponential quadratures, and that the accuracy is stable for a wide range of scaling parameters, α .^[31]

Procedure

We will define SG-2 and SG-3 parameters for the elements H through Cl, using the DE2 quadrature of eq. (6). We, therefore, need to specify a scaling parameter α as well as the number of Lebedev integration points contained in each radial shell, for each supported element, and these choices are discussed below. All calculations have been performed using a locally-modified version of Q-CHEM.^[34] For reasons discussed below, we have not pruned the grids for rare-gas elements, and we have also not investigated the pruning procedure for elements beyond Ar. For these cases, we simply define “SG-2” to be an unpruned (75,302) Euler–Maclaurin–Lebedev (EML) grid,^[26] and “SG-3” as an unpruned (99,590) EML grid. Quantum chemistry calculations involving a significant number of nuclei beyond Cl are relatively rare, therefore we do not view this as a significant limitation. For functionals such as ω B97X-V^[10] and ω B97M-V^[11] that include the non-local “VV10” van der Waals functional,^[18] the SG-1 grid is used to integrate VV10. This has been shown to be adequate.^[10]

Radial scaling factors

The scaling factor α is used to map $x \in (-\infty, +\infty)$ onto $r \in [0, +\infty)$. We select the value of α by insisting that the density integrate to the correct number of electrons, $N = \int \rho(\mathbf{r}) d\mathbf{r}$. These tests were performed at the ω B97X-V/aug-cc-pVTZ level of theory, where ω B97X-V is a hybrid GGA functional that is fairly sensitive to the quality of the integration grid.^[10] For each element X ranging from H to Ar, we tested scaling factors α in the range 1.0–3.2 and selected a value that accurately integrates the ground state density for both the atom X and its hydride HX.

Grid pruning

The pruning procedure consists in reducing the number of angular grid points in certain radial shells, namely, those that are close to the nucleus and those that are far from it, while generally preserving the number of angular grid points (at either $N_{\Omega} = 302$ or $N_{\Omega} = 590$, in this work) in the valence region of space. We developed this pruning procedure using the hydrides HX of all 18 elements through Ar. For rare-gas dimers, however, spurious oscillations in potential energy curves are present even when the *unpruned* (75,302) and (99,590) grids are used, especially for the Minnesota functionals, as shown for Ar₂ in Figure 1. Even in the case of the ω B97X-V functional, we were unable to obtain pruned grids that did not exacerbate this problem. Because of this, and due to the rarity of noble gas atoms in chemical applications, we choose not to prune the grids for the noble gas elements.

For the remaining elements H through Cl, we partition the integration grid into five or more concentric regions with several radial shells in each region. Each radial shell within a given region is required to have the same value of N_{Ω} , to simplify

Table 1. Lebedev partitions and scaling factors that define SG-2 and SG-3.^[a]

| Element | SG-2 | | | SG-3 | | |
|---------|------------------------------------|----------|--------------------|--|----------|--------------------|
| | Lebedev Partition | α | N_{total} | Lebedev Partition | α | N_{total} |
| H | $6^{35}110^{12}302^{16}86^7 26^5$ | 2.6 | 7094 | $6^{45}110^{16}590^{21}194^{10}50^7$ | 2.7 | 16710 |
| Li | $6^{35}110^{12}302^{17}86^7 50^4$ | 3.2 | 7466 | $6^{46}110^{16}590^{22}146^9 50^6$ | 3.0 | 16630 |
| Be | $6^{35}110^{12}302^{17}86^7 50^4$ | 2.4 | 7466 | $6^{42}86^6 110^{14}590^{22}194^3 146^6 50^6$ | 2.4 | 17046 |
| B | $6^{35}110^{12}302^{17}146^7 26^4$ | 2.4 | 7790 | $6^{42}86^6 110^{14}590^{22}194^9 50^6$ | 2.4 | 17334 |
| C | $6^{35}110^{12}302^{17}146^7 26^4$ | 2.2 | 7790 | $6^{46}146^6 16^5 590^{22}302^1 194^2 146^6 86^6$ | 2.4 | 17674 |
| N | $6^{35}110^{12}302^{17}86^7 26^4$ | 2.2 | 7370 | $6^{40}110^{18}590^{24}146^{11} 50^6$ | 2.4 | 18286 |
| O | $6^{30}110^{14}302^{18}146^8 50^5$ | 2.2 | 8574 | $6^{40}110^{14}194^2 302^2 590^{24}302^1 194^1 146^8 50^7$ | 2.6 | 18946 |
| F | $6^{26}110^{16}302^{19}110^8 50^6$ | 2.2 | 8834 | $6^{35}110^{17}194^4 590^{25}194^2 110^8 50^8$ | 2.1 | 19274 |
| Na | $6^{35}110^{12}302^{17}86^7 50^4$ | 3.2 | 7466 | $6^{46}110^{16}590^{22}146^9 50^6$ | 3.2 | 16630 |
| Mg | $6^{35}110^{12}302^{17}86^7 50^4$ | 2.4 | 7466 | $6^{48}110^{15}590^{20}146^7 50^9$ | 2.6 | 16532 |
| Al | $6^{32}110^{15}302^{17}146^7 86^4$ | 2.5 | 8342 | $6^{42}86^6 110^{14}590^{22}194^3 146^6 50^6$ | 2.6 | 17,046 |
| Si | $6^{32}110^{15}302^{17}146^7 50^4$ | 2.3 | 8342 | $6^{42}86^6 110^{14}590^{22}194^9 50^6$ | 2.8 | 17334 |
| P | $6^{30}110^{14}302^{17}146^7 38^7$ | 2.5 | 8142 | $6^{35}86^1 110^{18}194^4 590^{25}194^2 146^8 50^6$ | 2.4 | 19658 |
| S | $6^{30}110^{14}302^{17}146^7 38^7$ | 2.5 | 8142 | $6^{35}86^1 110^{18}194^4 590^{25}194^2 146^8 50^6$ | 2.4 | 19658 |
| Cl | $6^{26}110^{16}302^{19}110^8 50^6$ | 2.5 | 8834 | $6^{35}110^{17}194^4 590^{25}194^2 110^8 50^8$ | 2.6 | 19274 |

[a] For elements not listed here, we define SG-2 to be an unpruned (75,302) EML grid and SG-3 to be an unpruned (99,590) grid, whereas SG-2 and SG-3 are defined to use the "DE2" quadrature in eq. (6).

the pruning procedure, and this number is systematically reduced by carefully monitoring both the electronic energy and integrated density of the hydride HX, using the unpruned grid for the H atom in HX. In the case X = H (i.e., H₂ molecule), the pruned SG-2 grid results in a Lebedev partition that we write as

$$6^{35}110^{12}302^{16}86^7 26^5$$

The notation here indicates that the innermost 35 radial shells have 6 Lebedev points each, the next 12 radial shells have 110 angular points each, and so forth, with the outermost five radial shells each containing 26 Lebedev points. This pruned grid results in a total energy for H₂ that differs by only 1.6 μ Hartree from that of the unpruned (75,302) grid with the same value of α , but contains only 7094 points per H atom as compared to 22,650 points per atom for the unpruned grid. Similarly, for SG-3 the calculations on H₂ suggest a partition

$$6^{45}110^{16}590^{21}194^{10}50^7$$

that results in an error of 3 μ Hartree with respect to the unpruned (99,590) grid but reduces the number of points to 16,710 per H atom versus 58,410 for the unpruned grid. The parameters that define the SG-2 and SG-3 grids are listed in Table 1.

Results and Discussion

The remainder of this work is dedicated to benchmarking the accuracy of SG-2 and SG-3. For each property, we will compare SG-2 to an unpruned (75,302) EML grid and SG-3 to an unpruned (99,590) EML grid, with the difference defined as the "pruning error." Results obtained with the two unpruned EML grids will also be compared to those obtained using an unpruned (250,974) EML grid. We take the latter to be the benchmark-quality result, and define the difference as the "grid error."

Workhorse properties such as atomization energies, molecular geometries, and vibrational frequencies will be tested, along with other properties that are known to be especially sensitive to the quality of the grid. The latter include the description of near-degenerate isomers and degenerate vibrational frequencies, non-covalent interactions, and non-linear optical properties. The hybrid GGA functional ω B97X-V^[10] will be examined along with various Minnesota functionals^[13] and a meta-GGA representative from B97 suite, ω B97M-V.^[11] We find that the Minnesota functionals are especially sensitive to the quality of the integration grid (consistent with the findings in Ref. 9), and thus can serve as "worst-case scenarios" for grid-dependence and pruning. The aug-cc-pVTZ (aTZ) basis set is used unless indicated otherwise. All calculations were performed using a locally-modified version of Q-CHEM.^[34]

Atomization energies

Atomization energies for the G2 dataset,^[35] evaluated at the ω B97X-V/aTZ level of theory using various grids, are listed in Table 2. Calculations are performed using (75,302), (99,590), and (250,974) grids, as well as pruned counterparts of the former two, namely, SG-2 and SG-3, respectively. In terms of pruning errors (i.e., the energy difference between the pruned and unpruned results), the mean unsigned deviations (MUDs) are 0.03 kcal/mol for SG-2 and 0.01 kcal/mol for SG-3. Grid errors, which we define as the difference between either the (75,302) or the (99,590) result with respect to a (250,974) grid, are even smaller, with MUDs of <0.01 kcal/mol. This demonstrates that both the medium-quality and the high-quality grid are converged, with respect to calculation of atomization energies.

Analogous data computed at the M06-2X/aTZ and ω B97M-V/aTZ levels can be found in Tables S1 and S2 of the Supporting Information. At the M06-2X/aTZ level, the pruning errors exhibit MUDs of 0.09 kcal/mol (SG-2) and 0.03 kcal/mol (SG-3), while grid errors exhibit MUDs of 0.03 kcal/mol for (75,302)

Table 2. Atomization energies (in kcal/mol) at the ω B97X-V/aug-cc-pVTZ level.^[a]

| Molecule | Energy | | Error | | Energy | | Error | |
|-----------------------------------|--------|----------|------------------------|---------------------|--------|----------|------------------------|---------------------|
| | SG-2 | (75,302) | Pruning ^[b] | Grid ^[c] | SG-3 | (99,590) | Pruning ^[b] | Grid ^[c] |
| BeH | 683.19 | 683.19 | 0.00 | 0.00 | 683.19 | 683.19 | 0.00 | 0.00 |
| CH ₂ CH ₂ | 560.84 | 560.82 | -0.02 | 0.00 | 560.83 | 560.82 | -0.01 | 0.00 |
| CH ₂ O | 372.51 | 372.49 | -0.02 | 0.00 | 372.51 | 372.49 | -0.02 | 0.00 |
| CH ₂ (singlet) | 179.57 | 179.54 | -0.03 | 0.00 | 179.56 | 179.54 | -0.02 | 0.00 |
| CH ₂ (triplet) | 188.18 | 188.16 | -0.02 | 0.00 | 188.18 | 188.16 | -0.02 | 0.00 |
| CH ₃ CH ₃ | 711.42 | 711.39 | -0.03 | 0.00 | 711.41 | 711.39 | -0.02 | 0.00 |
| CH ₃ Cl | 394.64 | 394.58 | -0.06 | 0.00 | 394.59 | 394.58 | -0.01 | 0.00 |
| CH ₃ OH | 511.73 | 511.70 | -0.03 | 0.00 | 511.72 | 511.70 | -0.02 | 0.00 |
| CH ₃ | 306.39 | 306.36 | -0.03 | 0.00 | 306.38 | 306.36 | -0.02 | 0.00 |
| CH ₃ SH | 474.46 | 474.43 | -0.03 | -0.01 | 474.44 | 474.42 | -0.02 | 0.00 |
| CH ₄ | 418.65 | 418.66 | 0.01 | -0.01 | 418.65 | 418.66 | 0.01 | -0.01 |
| CH | 83.81 | 83.80 | -0.01 | 0.00 | 83.81 | 83.80 | -0.01 | 0.00 |
| Cl ₂ | 56.80 | 56.92 | 0.12 | 0.00 | 56.94 | 56.92 | -0.02 | 0.00 |
| ClF | 60.90 | 60.88 | -0.02 | 0.00 | 60.88 | 60.88 | 0.00 | 0.00 |
| ClO | 64.69 | 64.63 | -0.06 | 0.00 | 64.64 | 64.63 | -0.01 | 0.00 |
| CN | 173.64 | 173.62 | -0.02 | 0.00 | 173.62 | 173.62 | 0.00 | 0.00 |
| CO ₂ | 387.66 | 387.63 | -0.03 | 0.00 | 387.65 | 387.63 | -0.02 | 0.00 |
| CO | 256.18 | 256.15 | -0.03 | 0.00 | 256.17 | 256.15 | -0.02 | 0.00 |
| CS | 166.07 | 166.03 | -0.04 | 0.01 | 166.06 | 166.04 | -0.02 | 0.00 |
| F ₂ | 37.11 | 37.13 | 0.02 | 0.00 | 37.15 | 37.13 | -0.02 | 0.00 |
| H ₂ O | 229.76 | 229.75 | -0.01 | 0.00 | 229.75 | 229.75 | 0.00 | 0.00 |
| HCCH | 399.70 | 399.68 | -0.02 | 0.00 | 399.70 | 399.68 | -0.02 | 0.00 |
| HCl | 105.67 | 105.66 | -0.01 | 0.00 | 105.67 | 105.66 | -0.01 | 0.00 |
| HCN | 309.83 | 309.80 | -0.03 | 0.00 | 309.81 | 309.80 | -0.01 | 0.00 |
| HCO | 278.61 | 278.59 | -0.02 | 0.00 | 278.61 | 278.59 | -0.02 | 0.00 |
| HF | 138.40 | 138.38 | -0.02 | 0.00 | 138.40 | 138.38 | -0.02 | 0.00 |
| HOCl | 163.49 | 163.47 | -0.02 | 0.01 | 163.49 | 163.47 | -0.02 | 0.01 |
| HOOH | 267.21 | 267.19 | -0.02 | 0.00 | 267.20 | 267.19 | -0.01 | 0.00 |
| Li ₂ | 20.80 | 20.80 | 0.00 | 0.00 | 20.80 | 20.80 | 0.00 | 0.00 |
| LiF | 135.15 | 135.15 | 0.00 | 0.00 | 135.16 | 135.15 | -0.01 | 0.00 |
| LiH | 57.31 | 57.31 | 0.00 | 0.00 | 57.31 | 57.31 | 0.00 | 0.00 |
| N ₂ | 227.56 | 227.52 | -0.04 | 0.00 | 227.52 | 227.52 | 0.00 | 0.00 |
| Na ₂ | 15.68 | 15.68 | 0.00 | 0.00 | 15.68 | 15.68 | 0.00 | 0.00 |
| NaCl | 96.79 | 96.78 | -0.01 | 0.00 | 96.79 | 96.78 | -0.01 | 0.00 |
| NH ₂ NH ₂ | 439.40 | 439.37 | -0.03 | 0.00 | 439.38 | 439.37 | -0.01 | 0.00 |
| NH ₂ | 184.45 | 184.41 | -0.04 | 0.00 | 184.41 | 184.41 | 0.00 | 0.00 |
| NH ₃ | 298.26 | 298.25 | -0.01 | 0.00 | 298.25 | 298.25 | 0.00 | 0.00 |
| NH | 85.02 | 84.96 | -0.06 | 0.00 | 84.97 | 84.96 | -0.01 | 0.00 |
| NO | 156.54 | 156.54 | 0.00 | 0.00 | 156.55 | 156.54 | -0.01 | 0.00 |
| O ₂ | 123.92 | 123.89 | -0.03 | 0.00 | 123.91 | 123.89 | -0.02 | 0.00 |
| OH | 107.01 | 107.00 | -0.01 | 0.00 | 107.00 | 107.00 | 0.00 | 0.00 |
| P ₂ | 114.44 | 114.45 | 0.01 | 0.00 | 114.47 | 114.45 | -0.02 | 0.00 |
| PH ₂ | 158.06 | 158.05 | -0.01 | 0.00 | 158.05 | 158.05 | 0.00 | 0.00 |
| PH ₃ | 245.01 | 245.01 | 0.00 | 0.00 | 245.02 | 245.01 | -0.01 | 0.00 |
| S ₂ | 102.47 | 102.48 | 0.01 | 0.00 | 102.51 | 102.48 | -0.03 | 0.00 |
| SH ₂ | 182.96 | 182.94 | -0.02 | 0.00 | 182.95 | 182.94 | -0.01 | 0.00 |
| Si ₂ | 74.34 | 74.38 | 0.04 | -0.01 | 74.39 | 74.37 | -0.02 | 0.00 |
| SiH ₂ (singlet) | 153.75 | 153.71 | -0.04 | 0.00 | 153.72 | 153.71 | -0.01 | 0.00 |
| SiH ₂ (triplet) | 132.04 | 132.03 | -0.01 | 0.01 | 132.04 | 132.04 | 0.00 | 0.00 |
| SiH ₃ | 228.27 | 228.25 | -0.02 | 0.00 | 228.25 | 228.25 | 0.00 | 0.00 |
| SiH ₃ SiH ₃ | 537.48 | 537.43 | -0.05 | 0.00 | 537.44 | 537.43 | -0.01 | 0.00 |
| SiH ₄ | 324.67 | 324.65 | -0.02 | 0.00 | 324.66 | 324.65 | -0.01 | 0.00 |
| SiO | 186.18 | 186.14 | -0.04 | 0.01 | 186.16 | 186.15 | -0.01 | 0.00 |
| SO ₂ | 243.23 | 243.21 | -0.02 | 0.00 | 243.22 | 243.21 | -0.01 | 0.00 |
| SO | 123.98 | 123.93 | -0.05 | 0.00 | 123.95 | 123.93 | -0.02 | 0.00 |
| MUD ^[d] | | | 0.03 | 0.00 | | | 0.01 | 0.00 |

[a] Using MP2/6-31G* geometries. [b] Difference between pruned and unpruned results. [c] Difference with respect to a (250, 974) grid. [d] Mean unsigned deviation.

and < 0.01 kcal/mol for (99,590). In case of ω B97M-V/aTZ, the MUDs for pruning errors are 0.04 and 0.01 kcal/mol for SG-2 and SG-3, respectively, whereas the grid errors are both vanishingly small.

Isomerization energies

Large errors have been reported in isomerization energies for organic reactions when meta-GGAs from the Minnesota suite of functionals are used with low-quality grids.^[9] Here, we

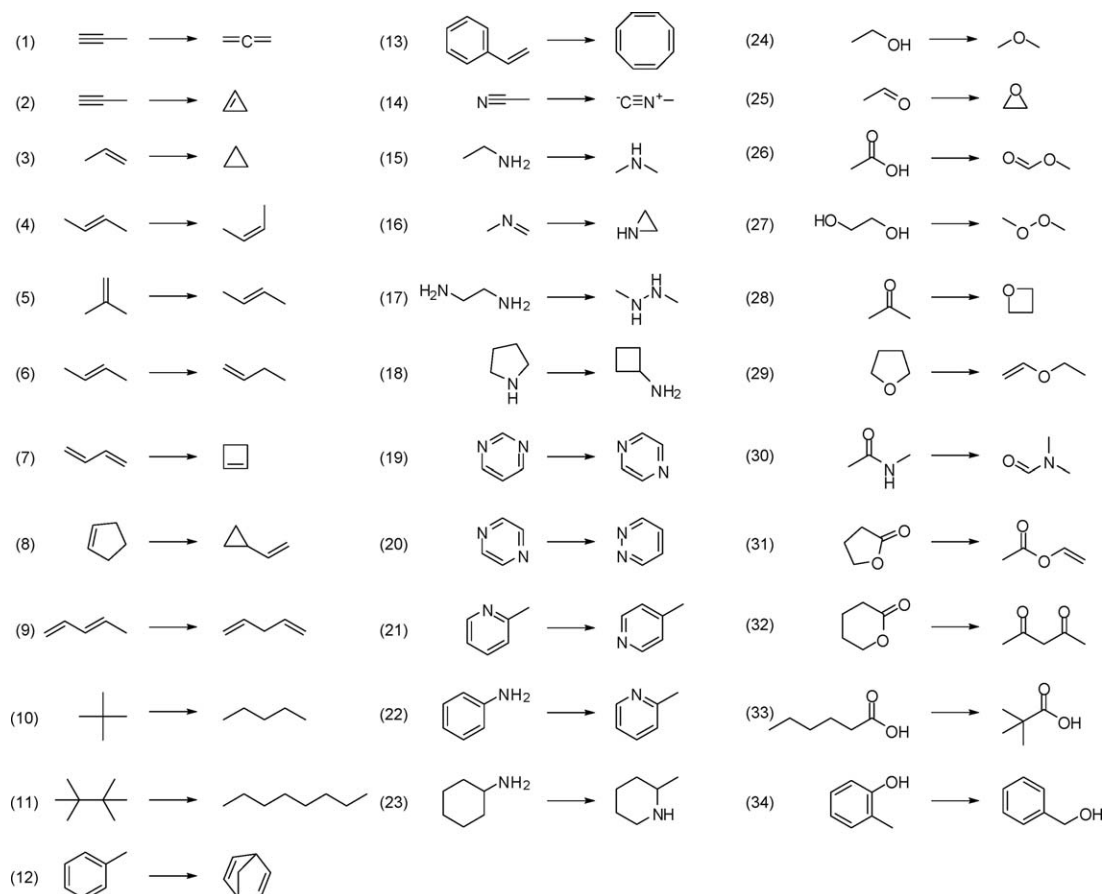


Figure 2. Test set of organic isomerization reactions. Reproduced with permission from Grimme et al., *J. Org. Chem.*, 2007, 72, 2118, copyright 2007 American Chemical Society.

compute isomerization energies for a set of 34 organic reactions assembled by Grimme et al.^[6] and used in the study in Ref. 9. The dataset consists of 13 reactions involving aliphatic and aromatic hydrocarbons (reactions 1–13 in Fig. 2), 10 reactions involving nitrogen atoms (reactions 14–23), and 11 involving oxygen atoms (reactions 24–34). Structures were optimized at B3LYP/TZV(d,p) level (SG-1 grid) and then single-point energy calculations were performed at the ω B97X-V/TZV(d,p) and ω B97M-V/TZV(d,p) levels using various integration grids. Results are presented in Tables 3 and Table S3 of the Supporting Information. In terms of MUDs, the pruning errors for both approaches are the same: 0.03 kcal/mol for SG-2 and 0.01 kcal/mol for SG-3. For ω B97X-V/TZV(d,p), grid errors amount to 0.01 kcal/mol for both the (75,302) and the (99,590) grid, while the corresponding values for ω B97M-V/TZV(d,p) are 0.04 kcal/mol (SG-2) and < 0.01 kcal/mol (SG-3).

As noted previously,^[24] an especially good test case for the pruning procedure is the neopentane \rightarrow *n*-pentane isomerization, reaction 10 in Figure 2. The experimental isomerization energy is only -1.2 kcal/mol, but because the two isomers have very different shapes, a DFT calculation of the relative energies of the two isomers can easily be overwhelmed by numerical error in the quadrature step. For SG-2 and SG-3, however, the pruning errors for this reaction are ≤ 0.1 kcal/mol in magnitude, consistent with the overall MUDs for the

isomerization test set, and small enough to reliably resolve the isomerization energy using the pruned grids.

Molecular geometries

Bond lengths and bond angles for a set of molecules representing the first three rows of the periodic table are presented in Tables 4 and S4 (in the Supporting Information). These parameters were optimized at the ω B97X-V/aTZ level (Table 4) and at the ω B97M-V/aTZ level (Supporting Information Table S4), using various integration grids. In terms of MUDs, the pruning errors for bond lengths are 0.0002 Å (SG-2) and 0.00006 Å (SG-3) at the ω B97X-V level. At the ω B97M-V level the pruning errors are only slightly larger, 0.0003 Å (SG-2) and 0.004 Å (SG-3). Pruning errors for bond angles using ω B97X-V/aTZ are 0.006° (SG-2) and 0.004° (SG-3), whereas using ω B97M-V/aTZ they are 0.033° (SG-2) and 0.018° (SG-3). The meta-GGA is consistently more sensitive to pruning in this case, but only slightly so. In all cases, the grid errors are significantly smaller than the pruning errors.

Vibrational frequencies

Harmonic vibrational frequencies for a set of molecules spanning the first three rows of the periodic table are presented in

Table 3. Isomerization energies (in kcal/mol) for organic reactions at the ω B97X-V/TZV(d,p) level.

| Rxn. ^[a] | Energy | | Error | | Energy | | Error | |
|---------------------|--------|----------|------------------------|---------------------|--------|----------|------------------------|---------------------|
| | SG-2 | (75,302) | Pruning ^[b] | Grid ^[c] | SG-3 | (99,590) | Pruning ^[b] | Grid ^[c] |
| 1 | -0.03 | -0.03 | 0.00 | -0.01 | 0.03 | 0.03 | 0.00 | -0.07 |
| 2 | 19.87 | 19.88 | 0.01 | 0.00 | 19.88 | 19.88 | 0.00 | 0.00 |
| 3 | 3.97 | 3.95 | -0.02 | 0.00 | 3.96 | 3.95 | -0.01 | 0.00 |
| 4 | 1.11 | 1.10 | -0.01 | -0.01 | 1.10 | 1.09 | -0.01 | 0.00 |
| 5 | 1.00 | 1.03 | 0.03 | 0.00 | 1.01 | 1.03 | 0.02 | 0.00 |
| 6 | 2.73 | 2.74 | 0.01 | -0.01 | 2.73 | 2.73 | 0.00 | 0.00 |
| 7 | 7.86 | 7.88 | 0.02 | 0.00 | 7.86 | 7.88 | 0.02 | 0.00 |
| 8 | 21.95 | 21.96 | 0.01 | 0.00 | 21.96 | 21.95 | -0.01 | 0.01 |
| 9 | 6.29 | 6.22 | -0.07 | 0.01 | 6.28 | 6.23 | -0.05 | 0.00 |
| 10 | 3.15 | 3.12 | -0.03 | -0.03 | 3.11 | 3.09 | -0.02 | 0.00 |
| 11 | -0.11 | -0.08 | 0.03 | 0.02 | -0.11 | -0.11 | 0.00 | 0.05 |
| 12 | 45.76 | 45.82 | 0.06 | -0.02 | 45.84 | 45.85 | 0.01 | -0.05 |
| 13 | 37.74 | 37.81 | 0.07 | 0.02 | 37.86 | 37.83 | -0.03 | 0.00 |
| 14 | 22.89 | 22.89 | 0.00 | 0.01 | 22.89 | 22.89 | 0.00 | 0.01 |
| 15 | 7.55 | 7.59 | 0.04 | -0.01 | 7.61 | 7.58 | -0.03 | 0.00 |
| 16 | 7.68 | 7.68 | 0.00 | 0.00 | 7.68 | 7.68 | 0.00 | 0.00 |
| 17 | 26.55 | 26.51 | -0.04 | 0.00 | 26.50 | 26.51 | 0.01 | 0.00 |
| 18 | 11.96 | 11.90 | -0.06 | 0.00 | 11.90 | 11.90 | 0.00 | 0.00 |
| 19 | 4.95 | 4.88 | -0.07 | -0.01 | 4.95 | 4.87 | -0.08 | 0.00 |
| 20 | 17.96 | 18.04 | 0.08 | 0.00 | 17.94 | 18.04 | 0.10 | 0.00 |
| 21 | 1.10 | 1.15 | 0.05 | 0.00 | 1.16 | 1.15 | -0.01 | 0.00 |
| 22 | 2.67 | 2.63 | -0.04 | 0.00 | 2.64 | 2.63 | -0.01 | 0.00 |
| 23 | 5.03 | 4.99 | -0.04 | 0.01 | 5.01 | 5.00 | -0.01 | 0.00 |
| 24 | 11.17 | 11.15 | -0.02 | 0.00 | 11.15 | 11.15 | 0.00 | 0.00 |
| 25 | 24.63 | 24.63 | 0.00 | 0.00 | 24.62 | 24.63 | 0.01 | 0.00 |
| 26 | 16.79 | 16.77 | -0.02 | 0.00 | 16.77 | 16.77 | 0.00 | 0.00 |
| 27 | 63.60 | 63.60 | 0.00 | -0.01 | 63.60 | 63.60 | 0.00 | -0.01 |
| 28 | 29.29 | 29.29 | 0.00 | 0.00 | 29.30 | 29.29 | -0.01 | 0.00 |
| 29 | 15.29 | 15.31 | 0.02 | 0.01 | 15.33 | 15.32 | -0.01 | 0.00 |
| 30 | 9.96 | 9.93 | -0.03 | 0.01 | 9.92 | 9.93 | 0.01 | 0.01 |
| 31 | 17.95 | 17.97 | 0.02 | 0.00 | 17.97 | 17.95 | -0.02 | 0.02 |
| 32 | 8.49 | 8.45 | -0.04 | -0.01 | 8.46 | 8.47 | 0.01 | -0.03 |
| 33 | 8.62 | 8.54 | -0.08 | 0.01 | 8.56 | 8.55 | -0.01 | 0.00 |
| 34 | 7.22 | 7.21 | -0.01 | 0.00 | 7.22 | 7.21 | -0.01 | 0.00 |
| MUD ^[d] | | | 0.03 | 0.01 | | | 0.01 | 0.01 |

[a] See Figure 2. [b] Difference between pruned and unpruned results. [c] Difference with respect to a (250,974) grid. [d] Mean unsigned deviation.

Tables 5 and S5 (in the Supporting Information), where they were computed at the M11/, ω B97X-V/, and ω B97M-V/aTZ levels of theory. Analytic Hessians are not available for these functionals in Q-CHEM, so frequencies were computed by finite difference of analytic energy gradients, and in Supporting Information Table S6 we compare analytic and finite-difference results for ω B97X-D/aTZ, where the analytic Hessian is available. With very few exceptions, the finite difference error is $< 1 \text{ cm}^{-1}$, and in most cases it is $< 0.1 \text{ cm}^{-1}$, thus validating the finite-difference approach. This is consistent with the results of a more thorough analysis of finite-difference errors, in Ref. 36.

Using the SG-2 grid, M11/aTZ frequencies (Table 5) afford a MUD for the pruning error of 7.15 cm^{-1} with a maximum pruning error of 32.5 cm^{-1} . These are actually smaller than the grid errors (MUD = 9.4 cm^{-1} and maximum of 52.2 cm^{-1}) obtained when the unpruned (75,302) results are compared to benchmark (250,974) results. This behavior is not observed for SG-3, for which pruning errors are comparable to those observed for SG-2 (MUD = 6.4 cm^{-1} and maximum error of 35.0 cm^{-1}), but the grid errors are much smaller. In terms of

the MUDs, ω B97X-D/aTZ results (Supporting Information Table S6) are roughly comparable to those for M11/aTZ.

While the average pruning and grid errors for these two functionals seem acceptable, it is nevertheless disturbing for M11 the unpruned (75,302) grid shows numerous errors on the order of $20\text{--}30 \text{ cm}^{-1}$ with respect to the very dense (250,974) grid, with an outlier of 52 cm^{-1} , although for the (99,590) grid the maximum error is 12 cm^{-1} . For ω B97X-D, grid errors of $\sim 20 \text{ cm}^{-1}$ are observed for both (75,302) and (99,590). These larger errors are primarily associated with B–H, S–H, P–H, and Si–H stretching vibrations.

In contrast, errors in vibrational frequencies at the ω B97X-V/aTZ level are quite small, with maximum pruning errors of only 0.7 cm^{-1} (SG-2) and 0.1 cm^{-1} (SG-3); see Table 5. The difference, relative to the aforementioned functionals, may arise from the fact that the exchange inhomogeneity correction factor in ω B97X-V is based on a lower-order—and therefore less oscillatory—series expansion in the reduced density gradient, as compared to ω B97X-D or any of the Minnesota functionals.^[10,15,37] The ω B97M-V meta-GGA functional also uses a low-order expansion, but it is an expansion in both the reduced

Table 4. Comparison of geometrical parameters^[a] optimized at the ω B97X-V/aug-cc-pVTZ level.

| Molecule | Parameter | Value | | Error | | Value | | Error | |
|---------------------------------|------------------------------------|-----------|-----------|------------------------|---------------------|-----------|-----------|------------------------|---------------------|
| | | SG-2 | (75,302) | Pruning ^[b] | Grid ^[c] | SG-3 | (99,590) | Pruning ^[b] | Grid ^[c] |
| H ₂ | r(HH) | 0.74345 | 0.74349 | 0.00004 | -0.00027 | 0.74346 | 0.74349 | 0.00003 | -0.00027 |
| Li ₂ | r(LiLi) | 2.50461 | 2.50482 | 0.00021 | 0.00348 | 2.50478 | 2.50481 | 0.00004 | 0.00349 |
| N ₂ | r(NN) | 1.09124 | 1.09128 | 0.00004 | -0.00001 | 1.09127 | 1.09128 | 0.00001 | -0.00001 |
| O ₂ | r(OO) | 1.19746 | 1.19738 | -0.00008 | 0.00002 | 1.19740 | 1.19739 | -0.00002 | 0.00001 |
| F ₂ | r(FF) | 1.37940 | 1.37957 | 0.00017 | 0.00002 | 1.37948 | 1.37957 | 0.00009 | 0.00002 |
| Si ₂ | r(SiSi) | 2.23042 | 2.23123 | 0.00081 | 0.00003 | 2.23110 | 2.23126 | 0.00016 | 0.00000 |
| P ₂ | r(PP) | 1.88464 | 1.88563 | -0.00001 | -0.01618 | 1.86971 | 1.86958 | -0.00013 | -0.00013 |
| S ₂ | r(SS) | 1.88586 | 1.88563 | -0.00023 | 0.00001 | 1.88586 | 1.88563 | -0.00023 | 0.00001 |
| Cl ₂ | r(ClCl) | 1.98787 | 1.98954 | 0.00167 | -0.00039 | 1.98871 | 1.98913 | 0.00042 | 0.00002 |
| SiH ₂ | r(SiH) | 1.52246 | 1.52249 | 0.00003 | 0.00001 | 1.52246 | 1.52249 | 0.00003 | 0.00001 |
| | ∠(HSiH) | 91.90527 | 91.91032 | 0.00505 | 0.00471 | 91.91273 | 91.91387 | 0.00114 | 0.00116 |
| CH ₃ OH | r(CH _a) | 1.09031 | 1.09031 | 0.00000 | 0.00000 | 1.09030 | 1.09031 | 0.00001 | 0.00000 |
| | r(CH _b) | 1.09605 | 1.09603 | -0.00002 | 0.00000 | 1.09603 | 1.09604 | 0.00001 | -0.00001 |
| | r(OH) | 0.95935 | 0.95936 | 0.00001 | 0.00000 | 0.95935 | 0.95936 | 0.00001 | 0.00000 |
| | ∠(OCH _a) | 106.84777 | 106.84498 | -0.00279 | 0.00065 | 106.84325 | 106.84680 | 0.00355 | -0.00117 |
| | ∠(COH) | 108.68299 | 108.70626 | 0.02327 | -0.00477 | 108.69277 | 108.70479 | 0.01202 | -0.00330 |
| | ∠(H _b CH _b) | 109.08834 | 109.08496 | -0.00338 | -0.00001 | 109.08843 | 109.08436 | -0.00407 | 0.00059 |
| | r(CO) | 1.42039 | 1.42032 | -0.00007 | 0.00001 | 1.42032 | 1.42031 | -0.00001 | 0.00002 |
| HCO | r(CO) | 1.17291 | 1.17291 | 0.00000 | -0.00001 | 1.17291 | 1.17291 | 0.00000 | -0.00001 |
| | r(OH) | 1.12245 | 1.12249 | 0.00004 | -0.00001 | 1.12246 | 1.12248 | 0.00002 | 0.00000 |
| | ∠(OCH) | 124.45806 | 124.45123 | -0.00683 | 0.00162 | 124.45142 | 124.45119 | -0.00023 | 0.00166 |
| NH ₂ NH ₂ | r(NN) | 1.42695 | 1.42690 | -0.00005 | 0.00002 | 1.42690 | 1.42689 | -0.00001 | 0.00003 |
| | r(NH _a) | 1.01103 | 1.01104 | 0.00001 | 0.00000 | 1.01103 | 1.01104 | 0.00001 | 0.00000 |
| | r(NH _b) | 1.01399 | 1.01399 | 0.00000 | 0.00000 | 1.01400 | 1.01399 | -0.00001 | 0.00000 |
| | ∠(NNH _b) | 112.20262 | 112.20249 | -0.00013 | -0.00270 | 112.20267 | 112.20249 | -0.00018 | -0.00270 |
| | ∠(NNH _a) | 108.00723 | 108.01348 | 0.00625 | -0.00219 | 108.01463 | 108.01557 | 0.00094 | -0.00428 |

[a] Bond lengths in Ångstroms and bond angles in degrees. [b] Difference between pruned and unpruned results. [c] Difference with respect to a (250,974) grid.

density gradient and also the reduced kinetic energy density, and the dependence of the latter can be expected to increase the grid sensitivity as compared to ω B97X-V. This is indeed the case for vibrational frequencies (see Supporting Information Table S5), although the errors are much smaller than those for M11 or ω B97X-D. For both SG-2 and SG-3, the MUD for pruning is 2 cm⁻¹ at the ω B97M-V level, with grid errors of 1 cm⁻¹. Maximum errors (either grid or pruning) are < 20 cm⁻¹ for SG-2 and < 10 cm⁻¹ for SG-3.

The ethynyl radical, C₂H, presents a particularly challenging test case due to the presence of a low-frequency degenerate bending mode, for which sparse quadrature grids sometimes result in one or more imaginary frequencies. We computed harmonic vibrational frequencies for C₂H using six different functionals and six integration grids each, including SG-0 and SG-1. The frequencies themselves are listed in Table 6 and the errors in Table 7. With the exception of the ω B97X-D functional, for which analytic Hessians are used, all of the frequency calculations are based on finite difference of analytic gradients.

For ω B97X-V/aTZ, the computed frequencies are roughly comparable across all seven integration grids, albeit with slightly larger grid errors for SG-0 and SG-1 as compared to SG-2 and SG-3. All four of these standard integration grids, however—including the lowest-quality one, SG-0—preserve the degeneracy between modes 1 and 2 to within 0.24 cm⁻¹, both for this functional and for

ω B97M-V. Restricting the discussion to just SG-2 and SG-3, both pruning and grid errors are < 2 cm⁻¹ for ω B97X-V and < 3 cm⁻¹ for ω B97M-V. For ω B97X-D, the pruning and grid errors are < 10 cm⁻¹, consistent with the greater sensitivity of this functional for a wider array for vibrational frequencies, and results obtained using SG-0 and SG-1 exhibit unacceptably larger errors.

Finally, the three Minnesota functionals considered in Tables 6 and 7 actually preserve the degeneracy to about the same precision as the B97-based functionals, but their absolute vibrational frequencies are much more strongly dependent on the integration grid, even as compared to ω B97X-D. Results using SG-0 and SG-1 are unacceptable, with M06-HF predicting several imaginary frequencies, but even for SG-2 and SG-2, M11 exhibits pruning errors of 30–40 cm⁻¹ and grid errors approaching 20 cm⁻¹.

Non-linear optical properties

Calculation of hyperpolarizability tensors is challenging because these quantities are quite sensitive to both the basis set and the treatment of electron correlation, and in DFT calculations they are sensitive to the quality of the integration grid as well.^[38] Here, we examine hyper-Rayleigh scattering intensities, β_{HRS} , and Raman depolarization ratios (RDRs), both of which are derived from the hyperpolarizability tensor, β . Let us assume that the incident light is propagating along the x direction and a harmonic of that light is scattered in the y

Table 5. Harmonic vibrational frequencies (ν , in cm^{-1}), and differences ($\Delta\nu$) engendered by pruning and grid errors.

| Molecule | M11/aug-cc-pVTZ | | | | | | ω B97X-V/aug-cc-pVTZ | | | | | |
|---------------------------------|-----------------|------------------------|---------------------|---------------|------------------------|---------------------|-----------------------------|------------------------|---------------------|---------------|------------------------|---------------------|
| | (75,302) Grid | | | (99,590) Grid | | | (75,302) Grid | | | (99,590) Grid | | |
| | ν | Error, $\Delta\nu$ | | ν | Error, $\Delta\nu$ | | ν | Error, $\Delta\nu$ | | ν | Error, $\Delta\nu$ | |
| | | Pruning ^[a] | Grid ^[b] | | Pruning ^[a] | Grid ^[b] | | Pruning ^[a] | Grid ^[b] | | Pruning ^[a] | Grid ^[b] |
| BH ₃ | 1139.02 | 3.10 | -0.66 | 1138.44 | 6.44 | -0.08 | 1154.92 | 0.05 | -0.13 | 1154.79 | 0.05 | 0.00 |
| | 1183.03 | 1.64 | 3.30 | 1183.22 | 7.07 | 3.11 | 1206.78 | 0.18 | 0.05 | 1206.79 | 0.05 | 0.04 |
| | 1183.85 | 1.37 | 2.52 | 1183.54 | 9.65 | 2.83 | 1206.79 | 0.19 | 0.04 | 1206.80 | 0.04 | 0.03 |
| | 2518.69 | -22.57 | -24.33 | 2497.31 | -12.68 | -2.95 | 2565.72 | -0.86 | -0.69 | 2565.01 | 0.00 | 0.02 |
| | 2662.36 | -23.45 | -23.75 | 2641.35 | -14.89 | -2.74 | 2697.00 | -0.82 | -0.66 | 2696.32 | 0.01 | 0.02 |
| 2662.68 | -23.14 | -24.06 | 2641.43 | -12.94 | -2.81 | 2697.01 | -0.83 | -0.67 | 2696.32 | 0.01 | 0.02 | |
| Cl ₂ | 574.49 | 3.44 | 16.35 | 594.88 | -0.44 | -4.04 | 590.40 | 0.93 | 1.28 | 592.25 | 1.40 | -0.57 |
| CO ₂ | 692.13 | -0.06 | -1.35 | 692.14 | -0.19 | -1.36 | 685.72 | 0.17 | 0.11 | 685.75 | 0.06 | 0.08 |
| | 692.13 | -0.06 | -1.34 | 692.14 | -0.18 | -1.35 | 685.72 | 0.18 | 0.11 | 685.75 | 0.07 | 0.08 |
| 1399.57 | 1.19 | 1.02 | 1400.02 | 0.75 | 0.57 | 1390.80 | 0.02 | -0.03 | 1390.77 | 0.01 | 0.00 | |
| 2429.55 | 1.90 | 1.38 | 2429.71 | 1.63 | 1.22 | 2423.97 | 0.02 | -0.04 | 2423.93 | -0.01 | 0.00 | |
| F ₂ | 1123.33 | 1.25 | 0.86 | 1124.41 | 1.54 | -0.22 | 1112.97 | 2.02 | -0.14 | 1112.61 | 1.47 | 0.22 |
| NH ₂ NH ₂ | 469.60 | -0.82 | -4.59 | 454.76 | -2.34 | 10.25 | 442.41 | 0.61 | -2.15 | 440.17 | 0.33 | 0.09 |
| | 796.65 | -1.51 | -9.59 | 785.34 | 1.97 | 1.72 | 831.07 | 0.39 | -0.75 | 830.20 | 0.23 | 0.12 |
| | 938.55 | -0.63 | -8.32 | 926.15 | 2.37 | 4.08 | 975.89 | 0.27 | -0.69 | 975.11 | 0.23 | 0.09 |
| | 1147.46 | -2.38 | -2.63 | 1145.37 | -3.23 | -0.54 | 1139.85 | -0.18 | -0.10 | 1139.74 | -0.05 | 0.01 |
| | 1291.32 | -0.59 | 0.75 | 1293.50 | -0.99 | -1.43 | 1308.50 | 0.03 | -0.35 | 1308.16 | -0.02 | -0.01 |
| | 1320.49 | -0.27 | -3.29 | 1317.07 | -0.48 | 0.13 | 1336.09 | 0.25 | 0.16 | 1336.18 | 0.07 | 0.07 |
| | 1662.88 | 1.40 | 1.18 | 1664.00 | 5.98 | 0.06 | 1681.88 | -0.02 | 0.05 | 1681.91 | -0.01 | 0.02 |
| | 1673.30 | 1.08 | 2.34 | 1675.35 | 5.62 | 0.29 | 1695.26 | 0.05 | -0.20 | 1695.12 | -0.01 | -0.06 |
| | 3527.52 | -6.51 | -2.94 | 3525.38 | -3.28 | -0.80 | 3511.68 | -0.66 | -0.42 | 3511.14 | 0.04 | 0.12 |
| | 3531.07 | -6.83 | -3.39 | 3528.43 | -2.11 | -0.75 | 3519.64 | -0.66 | -0.44 | 3519.09 | 0.05 | 0.11 |
| | 3627.25 | -8.07 | -4.07 | 3623.38 | -1.98 | -0.20 | 3608.97 | -0.74 | -0.56 | 3608.34 | 0.05 | 0.07 |
| | 3630.84 | -8.77 | -4.59 | 3626.36 | -2.26 | -0.11 | 3612.82 | -0.74 | -0.58 | 3612.19 | 0.05 | 0.05 |
| H ₂ O ₂ | 374.47 | -25.57 | 10.29 | 390.40 | -18.43 | -5.64 | 389.76 | -1.44 | 2.50 | 392.73 | -1.70 | -0.47 |
| | 1032.02 | -1.80 | 0.95 | 1033.01 | -0.31 | -0.04 | 1023.96 | 0.07 | 0.02 | 1024.03 | -0.04 | -0.05 |
| | 1342.32 | -3.96 | 11.16 | 1349.18 | -2.68 | 4.30 | 1356.23 | -0.40 | -0.67 | 1355.77 | -0.25 | -0.21 |
| | 1450.09 | 2.41 | 10.65 | 1461.89 | -2.34 | -1.15 | 1461.98 | 0.32 | -0.45 | 1461.68 | 0.17 | -0.15 |
| | 3817.11 | -3.50 | -3.00 | 3813.15 | -2.26 | 0.96 | 3813.21 | 1.42 | 0.43 | 3814.04 | -0.20 | -0.40 |
| | 3818.53 | -3.57 | -2.98 | 3814.38 | -2.16 | 1.17 | 3814.48 | 1.44 | 0.42 | 3815.30 | -0.21 | -0.40 |
| | 4365.49 | 3.93 | -0.26 | 4365.16 | 34.98 | 0.07 | 4439.50 | 0.26 | 0.00 | 4439.50 | 0.12 | 0.00 |
| H ₂ S | 1242.21 | -2.34 | -52.19 | 1199.22 | -1.98 | -9.20 | 1214.72 | 1.60 | 1.82 | 1216.91 | -0.08 | -0.37 |
| | 2744.09 | -6.23 | -11.17 | 2735.77 | -2.33 | -2.85 | 2758.87 | 1.13 | 1.07 | 2759.43 | 0.54 | 0.51 |
| | 2753.42 | -6.03 | -11.88 | 2743.98 | -2.15 | -2.44 | 2771.13 | 1.16 | 1.25 | 2772.03 | 0.48 | 0.35 |
| HCCH | 729.95 | 12.00 | -13.34 | 716.04 | 26.56 | 0.57 | 707.09 | 0.49 | 0.92 | 707.79 | 0.20 | 0.22 |
| | 729.95 | 12.03 | -13.32 | 716.05 | 26.56 | 0.58 | 707.12 | 0.49 | 0.93 | 707.82 | 0.20 | 0.23 |
| | 786.14 | 12.78 | -13.82 | 771.70 | 29.04 | 0.62 | 785.86 | 0.53 | 1.00 | 786.61 | 0.16 | 0.25 |
| | 786.15 | 12.78 | -13.83 | 771.70 | 29.04 | 0.62 | 785.88 | 0.52 | 0.99 | 786.62 | 0.17 | 0.25 |
| | 2107.86 | -9.09 | -10.09 | 2097.85 | 1.32 | -0.08 | 2096.08 | 0.08 | 0.00 | 2096.13 | -0.06 | -0.05 |
| | 3402.90 | -2.28 | -4.89 | 3399.11 | 11.12 | -1.10 | 3414.70 | -0.03 | -0.21 | 3414.55 | 0.07 | -0.06 |
| | 3521.34 | -3.57 | -5.91 | 3516.44 | 10.54 | -1.01 | 3525.27 | -0.02 | -0.19 | 3525.14 | 0.07 | -0.06 |
| N ₂ | 2531.94 | -3.04 | -5.25 | 2526.92 | 0.08 | -0.23 | 2488.13 | -0.13 | -0.24 | 2487.96 | -0.05 | -0.07 |
| | O ₂ | 1747.16 | -5.66 | -6.32 | 1741.68 | -0.61 | -0.84 | 1710.61 | 0.34 | 0.44 | 1711.03 | 0.11 |
| PH ₂ | 1138.74 | -0.52 | -22.07 | 1118.90 | -0.19 | -2.23 | 1132.78 | 2.06 | 0.81 | 1133.28 | -0.03 | 0.31 |
| | 2402.88 | 8.47 | 2.11 | 2405.99 | 2.76 | -1.00 | 2428.81 | 0.66 | 0.82 | 2429.59 | 0.02 | 0.04 |
| | 2413.41 | 9.74 | 0.07 | 2414.64 | 2.98 | -1.16 | 2437.18 | 0.05 | 0.53 | 2437.64 | 0.07 | 0.07 |
| S ₂ | 739.75 | 14.34 | 24.66 | 761.02 | 2.70 | 3.39 | 778.87 | 0.28 | -0.82 | 778.30 | -0.62 | -0.25 |
| SiH ₂ | 1001.53 | -6.93 | 11.40 | 1000.86 | -1.06 | 12.07 | 1033.14 | 2.57 | -1.98 | 1031.37 | 0.04 | -0.21 |
| | 2041.33 | 32.47 | 29.17 | 2069.91 | -0.35 | 0.59 | 2086.39 | 0.64 | -0.27 | 2086.40 | -0.01 | -0.28 |
| 2048.06 | 30.40 | 27.33 | 2073.73 | -0.17 | 1.66 | 2086.71 | 0.65 | -0.37 | 2086.66 | -0.07 | -0.32 | |
| MUD ^[c] | | 7.15 | 9.39 | | 6.43 | 1.97 | | 0.60 | 0.70 | | 0.20 | 0.12 |

[a] Difference between pruned and unpruned results. [b] Difference with respect to a (250,974) grid. [c] Mean unsigned deviation.

direction but polarized vertically along the z axis. Then β_{HRS}^2 is defined in an ensemble-averaged way as^[38]

$$\langle \beta_{\text{HRS}}^2 \rangle = \langle \beta_{\text{zzz}}^2 \rangle + \langle \beta_{\text{zxx}}^2 \rangle, \quad (10)$$

where β_{zzz} and β_{zxx} are elements of the β tensor. The RDR is defined as

$$\text{RDR} = \langle \beta_{\text{zzz}}^2 \rangle / \langle \beta_{\text{zxx}}^2 \rangle. \quad (11)$$

Evaluation of β requires functional derivatives $\delta^3 E_{\text{xc}} / \delta \rho^3$ that are not yet available in Q-CHEM for many of the latest meta-GGA functionals. As such, we will compute hyperpolarizabilities using a finite-field approach,^[39] with values of the electric field perturbation that range in magnitude from 0.0005 to 0.0065

Table 6. Harmonic vibrational frequencies for ethynyl radical.

| Method ^[b] | Grid | Frequency ^[a] (cm ⁻¹) | | | |
|-----------------------|-----------|--|----------------|---------|---------|
| | | Mode 1 | Mode 2 | Mode 3 | Mode 4 |
| ω B97X-D | SG-0 | 743.62 | 744.20 | 2104.92 | 3460.39 |
| | SG-1 | 590.98 | 591.08 | 2104.79 | 3469.05 |
| | SG-2 | 470.89 | 472.60 | 2107.55 | 3475.40 |
| | SG-3 | 474.46 | 476.51 | 2110.19 | 3471.22 |
| | (75,302) | 478.07 | 479.11 | 2108.84 | 3468.66 |
| | (99,590) | 484.86 | 484.96 | 2109.76 | 3470.42 |
| ω B97X-V | (250,974) | 484.92 | 485.01 | 2110.64 | 3471.53 |
| | SG-0 | 516.85 | 517.09 | 2119.40 | 3471.71 |
| | SG-1 | 509.04 | 509.14 | 2113.53 | 3464.41 |
| | SG-2 | 501.74 | 501.84 | 2119.96 | 3466.66 |
| | SG-3 | 502.79 | 502.90 | 2119.89 | 3466.66 |
| | (75,302) | 500.86 | 500.97 | 2119.84 | 3466.68 |
| ω B97M-V | (99,590) | 502.19 | 502.29 | 2119.98 | 3466.71 |
| | (250,974) | 502.67 | 502.78 | 2119.91 | 3466.66 |
| | SG-0 | 463.13 | 463.22 | 2114.22 | 3471.54 |
| | SG-1 | 484.71 | 484.78 | 2113.76 | 3466.55 |
| | SG-2 | 487.81 | 487.89 | 2115.23 | 3472.89 |
| | SG-3 | 486.40 | 486.47 | 2115.09 | 3472.28 |
| M05-2X | (75,302) | 488.15 | 488.22 | 2114.81 | 3474.51 |
| | (99,590) | 489.06 | 489.13 | 2114.96 | 3473.19 |
| | (250,974) | 489.41 | 481.49 | 2115.08 | 3473.10 |
| | SG-0 | 520.05 | 520.09 | 2148.42 | 3485.71 |
| | SG-1 | 509.28 | 509.39 | 2154.93 | 3624.28 |
| | SG-2 | 431.69 | 431.84 | 2132.98 | 3505.39 |
| M06-HF | SG-3 | 410.15 | 410.31 | 2130.90 | 3509.10 |
| | (75,302) | 430.74 | 430.93 | 2137.00 | 3513.10 |
| | (99,590) | 400.74 | 400.94 | 2131.21 | 3506.02 |
| | (250,974) | 400.42 | 402.51 | 2131.75 | 3505.47 |
| | SG-0 | 957.99i | 279.53 | 2160.85 | 3259.15 |
| | SG-1 | 907.38i | 895.84i | 2238.15 | 3748.52 |
| M11 | SG-2 | 667.01 | 667.06 | 2182.00 | 3506.99 |
| | SG-3 | 664.04 | 664.21 | 2179.47 | 3512.82 |
| | (75,302) | 656.01 | 656.06 | 2195.36 | 3509.63 |
| | (99,590) | 650.64 | 650.81 | 2095.05 | 3466.47 |
| | (250,974) | 633.64 | 633.89 | 2178.13 | 3498.22 |
| | SG-0 | 903.91 | 903.93 | 2148.81 | 3506.92 |
| M11 | SG-1 | 553.54 | 553.58 | 2134.35 | 3565.25 |
| | SG-2 | 624.32 | 624.36 | 2121.08 | 3467.21 |
| | SG-3 | 595.48 | 595.52 | 2119.93 | 3464.24 |
| | (75,302) | 585.71 | 585.75 | 2127.09 | 3457.09 |
| | (99,590) | 566.09 | 566.13 | 2119.17 | 3452.83 |
| | (250,974) | 565.90 | 565.95 | 2118.96 | 3451.70 |

[a] Imaginary frequencies are highlighted in boldface font. [b] Using the aug-cc-pVTZ basis set.

a.u. If the field strength is too high, terms beyond β contribute to the polarization, whereas if the field strength is too low then the result can be overwhelmed by numerical noise. Tests at the CCSD/aTZ level, where analytic expressions for the higher order derivatives are available in our code,^[40] suggest that a finite-field calculation of $\langle \beta_{\text{HRS}}^2 \rangle$ differs from the analytic result by about 0.09 a.u. for CH₃CN, while for the RDR the finite-field error is about 0.04 a.u. This establishes the level of accuracy that can be expected in finite-field calculations of these quantities.

We computed β_{HRS} and the depolarization ratio for the molecules CH₃CN, CH₃Cl, and CCl₄, which have been used in previous benchmark studies of DFT non-linear optical properties.^[38] Results are reported in Table 8. At the ω B97X-V/aTZ level, both the grid and the pruning errors are tiny, amounting to

no more than 0.03 a.u. (SG-2) or 0.01 a.u. (SG-3) for β_{HRS} . Similar pruning errors are encountered at the ω B97M-V/aTZ level. These deviations are well within the accuracy of the finite-field approach that was quoted above, thus the pruning and grid errors in these properties seems insignificant.

Pruning errors are larger at the M06-2X/aTZ level, amounting to 0.15 a.u. in β_{HRS} and 0.05–0.07 a.u. in the RDR. While this is larger than the anticipated finite-field error, we choose not to modify the pruned grids in an attempt to reduce these errors, because to do so might dramatically increase the cost to integrate better-behaved exchange-correlation functionals such as ω B97X-V and ω B97M-V. For SG-3 at least, grid error with respect to (250,974) results is comparable to the finite-field error in the case of M06-2X.

Non-covalent interaction energies

Non-covalent interactions are known to converge slowly with respect to the quality of the integration grid,^[7,8,10–12,15] because such interactions are associated with regions of space where the density itself is small but the density gradient is large.^[20] Spurious oscillations in potential energy curves, such as those demonstrated for Ar₂ in Figure 1, have been reported for other rare-gas dimers and for benzene dimer.^[7,8] In Figures 3 and 4 we plot potential energy curves for the π -stacked “sandwich” isomer of (C₆H₆)₂ along the face-to-face distance coordinate, computed using four different density functionals, the 6-311++G(3df,3pd) basis set, and various integration grids. The four functionals selected here were chosen because each performs reasonably well for non-covalent interaction energies.^[10,12,13,41,42] M06-2X, in particular, has been characterized as “perhaps the most broadly useful hybrid Minnesota functional” (along with MN15) in a recent benchmark study.^[12]

Unsurprisingly—but important to document, nonetheless—severe problems arise when M06-2X is used in conjunction with the SG-0 and SG-1 integration grids. As shown in Fig. S1 of the Supporting Information, these problems manifest in the form of multiple local minima with not-insignificant well depths. These oscillations are significantly smaller, although not altogether absent, when M06-2X is used in conjunction with the (75,302) grid (Fig. 3). The (95,590) results are nearly identical to the non-oscillatory (250,974) results, save for one very small oscillation evident between 4.0 and 4.2 Å. Given that the unpruned “parent” grids exhibit oscillations for M06-2X, it is a foregone conclusion that their pruned versions will as well, although SG-2 and SG-3 certainly perform far better than SG-0 or SG-1. Even in light of this example, we choose not to be any more conservative in the pruning procedure, and must therefore concede that only the very dense (250,974) integration grid affords a potential energy curve that is qualitatively correct at the M06-2X/6-311++G(3df,3pd) level, although the (99,590) grid comes close.

This is not true for (C₆H₆)₂ potential curves computed using ω B97X-D, ω B97M-V, and ω B97X-V, as shown in Figure 4. Two very slight inflection points between 4.0 and 4.4 Å can be observed when using the (75,302) integration grids, but otherwise there are no oscillations in these potential curves. With

Table 7. Errors in harmonic vibrational frequencies for ethynyl radical.

| Method ^[c] | Grid | Pruning Error ^[a] (cm ⁻¹) | | | Grid Error ^[b] (cm ⁻¹) | | |
|-----------------------|------|--|--------|--------|---|--------|--------|
| | | Mode 2 | Mode 3 | Mode 4 | Mode 2 | Mode 3 | Mode 4 |
| ω B97X-D | SG-0 | -171.45 | 4.03 | 12.28 | -87.25 | 1.74 | -1.14 |
| | SG-1 | -119.27 | -0.83 | -5.29 | 12.59 | -5.02 | 2.81 |
| | SG-2 | -6.51 | -1.29 | 6.74 | 5.90 | 1.80 | 2.87 |
| ω B97X-V | SG-3 | -8.54 | 0.43 | 0.80 | 0.06 | 0.88 | 1.11 |
| | SG-0 | -0.14 | 3.40 | -2.78 | -14.04 | -2.90 | -2.27 |
| | SG-1 | -3.03 | 6.17 | -0.61 | 9.39 | 0.19 | -1.64 |
| ω B97M-V | SG-2 | 0.87 | 0.12 | -0.02 | 1.81 | 0.07 | -0.02 |
| | SG-3 | 0.61 | -0.09 | -0.05 | 0.49 | -0.07 | -0.05 |
| | SG-0 | 33.97 | -10.82 | 2.27 | -7.7 | 11.68 | -0.71 |
| M05-2X | SG-1 | 0.14 | 0.04 | 0.37 | 4.57 | 1.28 | 6.18 |
| | SG-2 | 0.33 | -0.42 | 1.62 | 1.27 | 0.27 | -1.41 |
| | SG-3 | 2.66 | -0.13 | 0.91 | 0.36 | 0.12 | -0.09 |
| M11 | SG-0 | -322.37 | -20.12 | -48.10 | 202.74 | 3.31 | 67.85 |
| | SG-1 | -58.79 | -1.05 | -5.19 | 165.67 | 24.23 | 124.00 |
| | SG-2 | 0.91 | -4.02 | -7.71 | -28.42 | -5.25 | -7.63 |
| M11 | SG-3 | -9.37 | -1.77 | -3.08 | -0.32 | 0.54 | -0.55 |
| | SG-0 | -415.88 | -20.37 | -69.62 | 77.87 | -2.24 | 18.90 |
| | SG-1 | 25.42 | -1.69 | 5.99 | -37.79 | 17.08 | 107.56 |
| M11 | SG-2 | 38.61 | -6.01 | 10.12 | -19.80 | -8.13 | -5.39 |
| | SG-3 | 29.39 | 0.76 | 11.43 | -0.18 | -0.21 | -1.13 |

[a] Difference between pruned and results. [b] Difference with respect to a (250,974) grid. [c] Using the aug-cc-pVTZ basis set.

the exception of the SG-2 grid for ω B97M-V, where the interaction energy differs from the (75,302) result by about 0.1 kcal/mol in the vicinity of the minimum, the potential curves for the pruned grids tracked the unpruned ones quite closely. SG-3 potential energy curves are converged with respect to (250,974) benchmarks. Given other numerical and basis-set-dependence problems with Minnesota functionals documented here and elsewhere,^[15] we are content to achieve such good performance with B97-based functionals, despite the problems for M06-2X.

The benzene and argon dimer examples demonstrate that non-covalent interactions place especially stringent demands on the integration grid, when full potential energy curves are

desired. At the same time, it is useful to know how various grids perform for intermolecular interaction energies computed at a decent approximation of the minimum-energy geometry. To investigate this, we computed interaction energies for the S66 set of non-covalent dimers^[43] using the M06-2X/, ω B97X-V/, and ω B97M-V/aTZ methods. Grid errors and pruning errors for all 66 complexes and all three methods, using both SG-2 and SG-3, appear in Tables S7–S9 in the Supporting Information. The MUD for the grid error is ≤ 0.02 kcal/mol for all three methods, and even for M06-2X where the pruning errors are largest, the MUD for pruning is 0.11 kcal/mol for SG-2 and 0.03 kcal/mol for SG-3. The maximum pruning error for this functional is 0.9 kcal/mol for SG-2 and 0.3 kcal/mol for SG-3.

Even for M06-2X and ω B97M-V, where SG-2 potential curves for benzene dimer are clearly not converged to the dense-grid

Table 8. Hyperpolarizability-derived quantities β_{HRS} and the Raman depolarization ratio (RDR), both in atomic units.^[a]

| Functional | Grid | CH ₃ CN | | CH ₃ Cl | | CCl ₄ | |
|-----------------|-----------|----------------------|------|----------------------|------|----------------------|------|
| | | β_{HRS} | RDR | β_{HRS} | RDR | β_{HRS} | RDR |
| M06-2X | SG-2 | 10.25 | 3.49 | 8.91 | 1.52 | 5.45 | 1.50 |
| | (75,302) | 10.12 | 3.42 | 8.88 | 1.50 | 5.41 | 1.50 |
| | SG-3 | 9.89 | 3.26 | 8.51 | 1.49 | 5.36 | 1.50 |
| | (99,590) | 9.81 | 3.21 | 8.64 | 1.52 | 5.28 | 1.50 |
| ω B97X-V | (250,974) | 9.79 | 3.20 | 8.61 | 1.50 | 5.22 | 1.50 |
| | SG-2 | 16.64 | 5.42 | 17.23 | 1.50 | 16.87 | 1.50 |
| | (75,302) | 16.61 | 5.41 | 17.21 | 1.50 | 16.85 | 1.50 |
| | SG-3 | 16.61 | 5.41 | 17.22 | 1.50 | 16.85 | 1.50 |
| ω B97M-V | (99,590) | 16.61 | 5.41 | 17.22 | 1.50 | 16.84 | 1.50 |
| | (250,974) | 16.61 | 5.41 | 17.22 | 1.50 | 16.83 | 1.50 |
| | SG-2 | 14.24 | 4.87 | 15.04 | 1.51 | 12.46 | 1.50 |
| | (75,302) | 14.26 | 4.82 | 15.07 | 1.50 | 12.50 | 1.50 |
| ω B97M-V | SG-3 | 14.26 | 4.81 | 15.06 | 1.50 | 12.49 | 1.50 |
| | (99,590) | 14.28 | 4.81 | 15.08 | 1.50 | 12.51 | 1.50 |
| | (250,974) | 14.28 | 4.81 | 15.08 | 1.50 | 12.52 | 1.50 |

[a] All calculations performed using the aug-cc-pVTZ basis set.

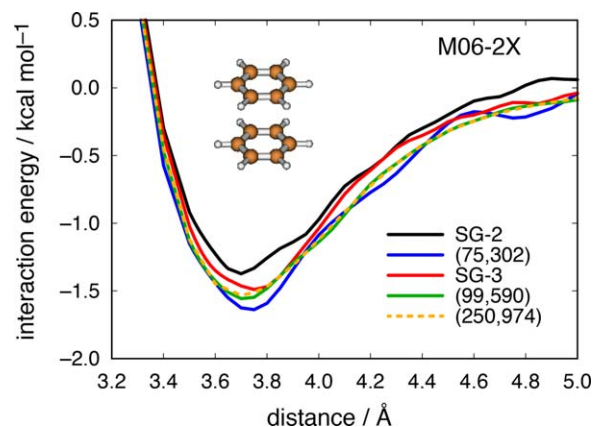


Figure 3. Potential energy curves for the "sandwich" isomer of (C₆H₆)₂ along the face-to-face distance coordinate computed at the M06-2X/6-311++G(3df,3pd) level using various integration grids. [Color figure can be viewed at wileyonlinelibrary.com]

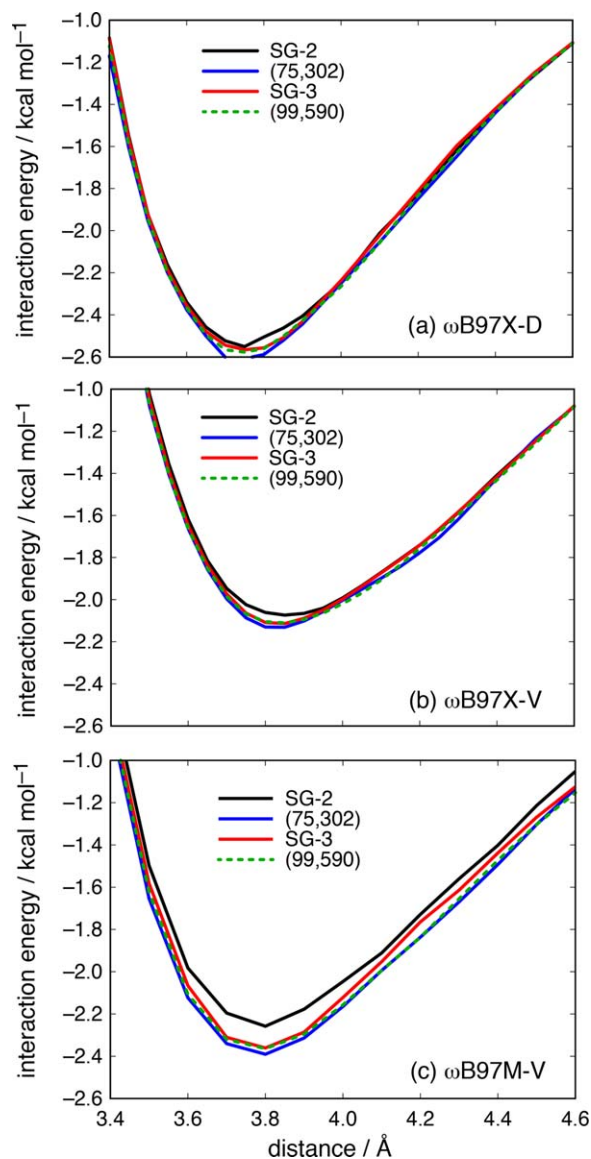


Figure 4. Potential energy curves for the “sandwich” isomer of $(C_6H_6)_2$ along the face-to-face distance coordinate, using (a) $\omega B97X-D$, (b) $\omega B97X-V$, and (c) $\omega B97M-V$. The 6-311++G(3df,3pd) basis set is used in each case. Benchmark (250,974) results are indistinguishable from (99,590) results, so the latter are omitted. [Color figure can be viewed at wileyonlinelibrary.com]

limit, errors in the SG-2 interaction energies are small, e.g., about 4% near the minimum, in the case of $\omega B97M-V$. This, combined with results for S66 suggests that SG-2 may be sufficient for non-covalent interaction energies. However, full potential energy curves for Ar_2 and for $(C_6H_6)_2$ obtained using Minnesota functionals caution against being too cavalier with the integration grids that are used in these cases. A reasonable geometry must first be located, which might be problematic for Ar_2 using M06-2X with anything short of the (250,974) integration grid. Overall, the pruning procedure for SG-2 and SG-3 seems quite faithful for non-covalent interaction energies where geometries are available, although oscillations in potential energy curves for the Minnesota functionals could make geometry optimization challenging in some cases.

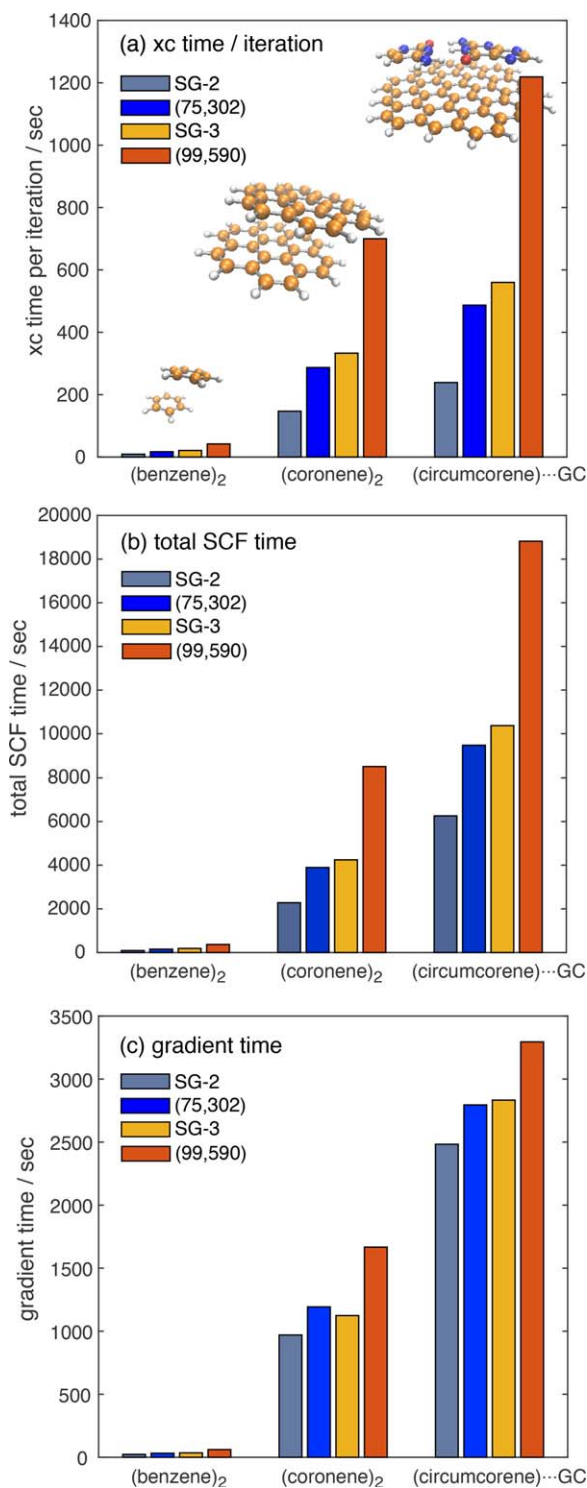


Figure 5. Timings for M06-2X/6-31G* calculations on three non-covalent complexes: benzene dimer, with 204 basis functions; coronene dimer, with 768 basis functions; and a complex of circumcoronene with a guanine-cytosine (GC) base pair, having 1151 basis functions. Shown are: (a) the average time per SCF iteration needed to evaluate the exchange-correlation energy [eq. (1)], (b) the total time required to evaluate the SCF energy, and (c) the total time required to evaluate the SCF energy gradient. All calculations were performed on a single processor. [Color figure can be viewed at wileyonlinelibrary.com]

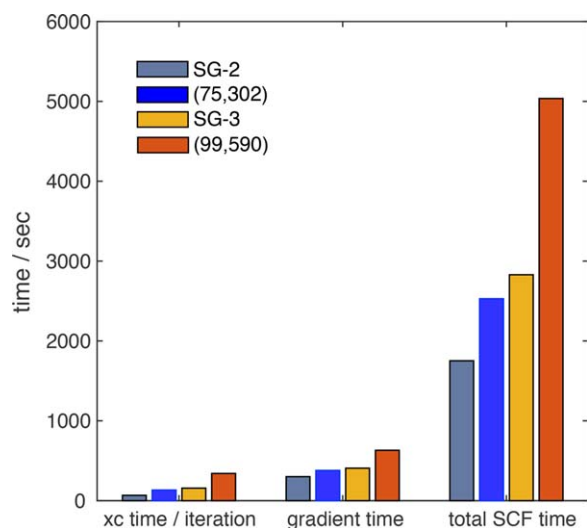


Figure 6. Timings for B97M-V/6-311++G(3df,3pd) calculations on benzene dimer. [Color figure can be viewed at wileyonlinelibrary.com]

Rotational invariance

Strictly speaking, the numerical integration step need not afford energies that are invariant with respect to rigid rotation of the entire molecule, although any violation of rotational invariance should become numerically insignificant in the limit of a sufficiently dense integration grid. To check whether the pruning procedure has exacerbated violations of rotational invariance, we recomputed the isomerization energies for several of the reactions in Figure 2 following several different overall rigid rotations of both the reactant and product species. Results in Table S10 in the Supporting Information demonstrate that these rotations change isomerization energies by at most 0.01 kcal/mol (and usually less), such that rotational invariance is preserved to high accuracy using SG-2 and SG-3.

Timings

Finally, we compare timings for the pruned versus unpruned grids, using as examples several non-covalent complexes from Ref. 44. Timing data for M06-2X/6-31G* calculations on a single processor are shown in Figure 5. A twofold speedup is realized in the exchange–correlation quadrature time for both SG-2 and SG-3, relative to the corresponding unpruned grids, in systems ranging in size from $(C_6H_6)_2$ up to (circumcoronene)··(guanine)··(cytosine). The total time required to evaluate the SCF energy also decreases on pruning, by factors ranging from 1.5 to 2.0, which in part shows that pruning does not lead to an increase in the number of SCF cycles required to reach convergence. Derivatives of Hartree-Fock exchange integrals for M06-2X become a significant bottleneck in evaluating the analytic energy gradient, which explains why the speedups in the gradient (see Fig. 5c) are not as significant as those obtained for the SCF energy.

Given that M06-2X contains Hartree-Fock exchange, evaluation of which becomes the most expensive step in building the Fock matrix for large systems, the speedups engendered by these new grids should be even more pronounced when using a functional that does not contain Hartree-Fock

exchange. Indeed, the situation changes dramatically when using the non-hybrid meta-GGA functional B97M-V,^[19] as shown in timing data for $(C_6H_6)_2$ in Figure 6. We continue to obtain a twofold speed-up in the exchange–correlation quadrature and a factor of 1.5–2.0 speedup in the total SCF time, but the speedup in the gradient evaluation is significantly larger as compared to M06-2X, amounting to a factor of 1.25 for SG-2 and 1.55 for SG-3.

Conclusions

We have introduced standard DFT integration grids of medium and high quality, based on pruned versions of $(N_r, N_\Omega) = (75, 302)$ and $(99, 590)$ integration grids, with a double-exponential quadrature for the radial part and Lebedev quadrature for the angular part. These grids extend the SG-0, SG-1, ... sequence into a regime that is suitable for integrating modern meta-GGA functionals. Equally importantly, they do so in a way that can easily be made reproducible across electronic structure codes, as the grid points are fully specified in this work. The SG-2 grid contains only about one-third as many points per atom as its parent $(75, 302)$ grid, while SG-3 removes an even greater fraction of the grid points as compared to its parent $(99, 590)$ grid. This yields significant cost savings, amounting to about a twofold speed up for the exchange–correlation part quadrature step, and a speedup of 1.5–2.0 in the total SCF time for systems ranging in size from 200 to 1150 basis functions. At the same time, the loss in accuracy (with respect to the unpruned parent grids) is minimal, and has been characterized here via calculations of atomization energies, optimized geometries, isomerization energies, vibrational frequencies, hyperpolarizabilities, and non-covalent interaction energies. In each case, the pruning error is much smaller than the precision needed to make chemically-informative statements about the quantities in question.


Based on our experience, we recommend use of the SG-3 grid for the particularly-sensitive Minnesota functionals, and also for functionals that contain B95. The SG-2 grid seems to suffice for most other meta-GGAs and for B97-based functionals, whose exchange enhancement factors are challenging to integrate. For other GGA functionals, SG-1 is adequate. A caveat to these recommendations is warranted, however, in the case of non-covalent interactions. For non-covalent interaction energies computed at known, minimum-energy geometries, the recommended grids engender negligible error, in most cases, as compared to our benchmark $(250, 974)$ grid, but potential energy curves may still exhibit spurious oscillations, especially for Minnesota functionals. This means that grids denser than our recommendations may be necessary for geometry optimizations and vibrational frequency calculations involving non-bonded interactions.

Acknowledgments

We thank Narbe Mardirossian for advice regarding the grid sensitivity of various functionals. Calculations were performed at the Ohio Supercomputer Center under project PAA-0003.^[45]

Keywords: density functional theory · numerical quadrature · pruned grids · meta-GGA · Minnesota functionals

How to cite this article: S. Dasgupta, J. M. Herbert *J. Comput. Chem.* **2017**, *38*, 869–882. DOI: 10.1002/jcc.24761

 Additional Supporting Information may be found in the online version of this article.

- [1] V. I. Lebedev, *Zh. vychisl. Mat. Mat. Fiz.* **1975**, *16*, 293.
 [2] V. I. Lebedev, *USSR Comp. Math. Math. Phys.* **1975**, *15*, 44.
 [3] W. Koch, M. C. Holthausen, *A Chemist's Guide to Density Functional Theory*, 2nd ed.; Wiley-VCH: New York, **2001**.
 [4] P. M. W. Gill, B. G. Johnson, J. A. Pople, *Chem. Phys. Lett.* **1993**, *209*, 506.
 [5] J. Gräfenstein, D. Cremer, *J. Chem. Phys.* **2007**, *127*, 164113.
 [6] S. Grimme, M. Steinmetz, M. Korth, *J. Org. Chem.* **2007**, *72*, 2118.
 [7] E. R. Johnson, R. A. Wolkow, G. A. DiLabio, *Chem. Phys. Lett.* **2004**, *394*, 334.
 [8] E. R. Johnson, A. D. Becke, C. D. Sherrill, G. A. DiLabio, *J. Chem. Phys.* **2009**, *131*, 034111.
 [9] S. E. Wheeler, K. N. Houk, *J. Chem. Theory Comput.* **2010**, *6*, 395.
 [10] N. Mardirossian, M. Head-Gordon, *Phys. Chem. Chem. Phys.* **2014**, *16*, 9904.
 [11] N. Mardirossian, M. Head-Gordon, *J. Chem. Phys.* **2016**, *144*, 214110.
 [12] N. Mardirossian, M. Head-Gordon, *J. Chem. Theory Comput.* **2016**, *12*, 4303.
 [13] Y. Zhao, D. G. Truhlar, *Theor. Chem. Acc.* **2008**, *120*, 215.
 [14] Y. Zhao, D. G. Truhlar, *Chem. Phys. Lett.* **2011**, *502*, 1.
 [15] N. Mardirossian, M. Head-Gordon, *J. Chem. Theory Comput.* **2013**, *9*, 4453.
 [16] M. Dion, H. Rydberg, E. Schröder, D. C. Langreth, B. I. Lundqvist, *Phys. Rev. Lett.* **2004**, *92*, 246401.
 [17] K. Lee, É. D. Murray, L. Kong, B. I. Lundqvist, D. C. Langreth, *Phys. Rev. B* **2010**, *82*, 081101.
 [18] O. A. Vydrov, T. Van Voorhis, *J. Chem. Phys.* **2010**, *133*, 244103.
 [19] N. Mardirossian, M. Head-Gordon, *J. Chem. Phys.* **2015**, *142*, 074111.
 [20] E. R. Johnson, S. Keinan, P. Mori-Sánchez, J. Contreras-García, A. J. Cohen, W. Yang, *J. Am. Chem. Soc.* **2010**, *132*, 6498.
 [21] M. E. Lasinski, N. A. Romero, S. T. Brown, J. P. Blaudeau, *J. Comput. Chem.* **2012**, *33*, 723.
 [22] For online documentation for the GAMESS program, Available at: http://www.msg.ameslab.gov/games/GAMESS_Manual/input.pdf, accessed on November 17, **2016**.
 [23] For online documentation for the Gaussian program, Available at: http://www.gaussian.com/g_tech/g_ur/k_integral.htm, accessed on November 17, **2016**.
 [24] S. H. Chien, P. M. W. Gill, *J. Comput. Chem.* **2006**, *27*, 730.
 [25] A. D. Becke, *J. Chem. Phys.* **1988**, *88*, 2547.
 [26] C. W. Murray, N. C. Handy, G. J. Laming, *Mol. Phys.* **1993**, *78*, 997.
 [27] O. Treutler, R. Ahlrichs, *J. Chem. Phys.* **1995**, *102*, 346.
 [28] M. E. Mura, P. J. Knowles, *J. Chem. Phys.* **1996**, *104*, 9848.
 [29] R. Lindh, P. Malmqvist, L. Gagliardi, *Theor. Chem. Acc.* **2001**, *106*, 178.
 [30] M. Mitani, *Theor. Chem. Acc.* **2011**, *130*, 645.
 [31] M. Mitani, Y. Yoshioka, *Theor. Chem. Acc.* **2012**, *131*, 1169.
 [32] H. Takahasi, M. Mori, *Publ. RIMS Kyoto Univ.* **1974**, *9*, 721.
 [33] M. Mori, *Publ. RIMS Kyoto Univ.* **2005**, *41*, 897.
 [34] Y. Shao, Z. Gan, E. Epifanovsky, A. T. B. Gilbert, M. Wormit, J. Kussmann, A. W. Lange, A. Behn, J. Deng, X. Feng, D. Ghosh, M. Goldey, P. R. Horn, L. D. Jacobson, I. Kaliman, R. Z. Khaliullin, T. Kúš, A. Landau, J. Liu, E. I. Proynov, Y. M. Rhee, R. M. Richard, M. A. Rohrdanz, R. P. Steele, E. J. Sundstrom, H. L. Woodcock, III, P. M. Zimmerman, D. Zuev, B. Albrecht, E. Alguire, B. Austin, G. J. O. Beran, Y. A. Bernard, E. Berquist, K. Brandhorst, K. B. Bravaya, S. T. Brown, D. Casanova, C. M. Chang, Y. Chen, S. H. Chien, K. D. Closser, D. L. Crittenden, M. Diedenhofen, R. A. DiStasio, Jr., H. Do, A. D. Dutoi, R. G. Edgar, S. Fatehi, L. Fusti-Molnar, A. Ghysels, A. Golubeva-Zadorozhnaya, J. Gomes, M. W. D. Hanson-Heine, P. H. P. Harbach, A. W. Hauser, E. G. Hohenstein, Z. C. Holden, T. C. Jagau, H. Ji, B. Kaduk, K. Khistyayev, J. Kim, J. Kim, R. A. King, P. Klunzinger, D. Kosenkov, T. Kowalczyk, C. M. Krauter, K. U. Lao, A. Laurent, K. V. Lawler, S. V. Levchenko, C. Y. Lin, F. Liu, E. Livshits, R. C. Lochan, A. Luenser, P. Manohar, S. F. Manzer, S. P. Mao, N. Mardirossian, A. V. Marenich, S. A. Maurer, N. J. Mayhall, C. M. Oana, R. Olivares-Amaya, D. P. O'Neill, J. A. Parkhill, T. M. Perrine, R. Peverati, P. A. Pieniazek, A. Prociuk, D. R. Rehn, E. Rosta, N. J. Russ, N. Sergueev, S. M. Sharada, S. Sharma, D. W. Small, A. Sodt, T. Stein, D. Stück, Y. C. Su, A. J. W. Thom, T. Tsuchimochi, L. Vogt, O. Vydrov, T. Wang, M. A. Watson, J. Wenzel, A. White, C. F. Williams, V. Vanovschi, S. Yeganeh, S. R. Yost, Z. Q. You, I. Y. Zhang, X. Zhang, Y. Zhao, B. R. Brooks, G. K. L. Chan, D. M. Chipman, C. J. Cramer, W. A. Goddard, III, M. S. Gordon, W. J. Hehre, A. Klamt, H. F. Schaefer, III, M. W. Schmidt, C. D. Sherrill, D. G. Truhlar, A. Warshel, X. Xu, A. Aspuru-Guzik, R. Baer, A. T. Bell, N. A. Besley, J. D. Chai, A. Dreuw, B. D. Dunietz, T. R. Furlani, S. R. Gwaltney, C. P. Hsu, Y. Jung, J. Kong, D. S. Lambrecht, W. Liang, C. Ochsenfeld, V. A. Rassolov, L. V. Slipchenko, J. E. Subotnik, T. Van Voorhis, J. M. Herbert, A. I. Krylov, P. M. W. Gill, M. Head-Gordon, *Mol. Phys.* **2015**, *113*, 184.
 [35] L. A. Curtiss, K. Raghavachari, G. W. Trucks, J. A. Pople, *J. Chem. Phys.* **1991**, *94*, 7221.
 [36] K.-Y. Liu, J. Liu, J. M. Herbert, Accuracy of finite-difference harmonic frequencies in density functional theory, submitted.
 [37] J. D. Chai, M. Head-Gordon, *J. Chem. Phys.* **2008**, *128*, 084106.
 [38] F. Castet, B. Champagne, *J. Chem. Theory Comput.* **2012**, *8*, 2044.
 [39] G. R. J. Williams, *J. Mol. Struct. (Theochem)* **1987**, *151*, 215.
 [40] K. D. Nanda, A. I. Krylov, *J. Chem. Phys.* **2016**, *145*, 204116.
 [41] K. U. Lao, J. M. Herbert, *J. Phys. Chem. A* **2015**, *119*, 235.
 [42] K. U. Lao, R. Schäffer, G. Jansen, J. M. Herbert, *J. Chem. Theory Comput.* **2015**, *11*, 2473.
 [43] J. Řezáč, K. E. Riley, P. Hobza, *J. Chem. Theory Comput.* **2011**, *7*, 2427.
 [44] Benchmark Energy and Geometry Database. Available at: <http://www.begdb.com>, accessed on November 17, **2016**.
 [45] Ohio Supercomputer Center. Available at: <http://osc.edu/ark:/19495/f5s1ph73>, accessed on November 17, **2016**.

Received: 19 November 2016

Revised: 25 January 2017

Accepted: 30 January 2017

Published online on 24 February 2017